

Scientific paper

Kinetics and Mechanism of Ligand Exchange Reaction of Copper(II) Complexes with Tetradentate Schiff Base Ligands

Rasoul Vafazadeh* and Somayeh Bidaki

Department of Chemistry, Yazd University, Yazd, Iran

* Corresponding author: E-mail: rvafazadeh@yazduni.ac.ir

Received: 10-12-2013

Abstract

The kinetics of a ligand exchange in the $\text{CuL}^4/\text{H}_2\text{L}^n$ system, where H_2L^n is the N,N' -alkylen-bis(salicyldimine) tetradentate Schiff base ligand ($n = 2$ or 3 , CH_2 groups in the chain length of the amine backbone) was studied spectrophotometrically in DMF solvent with or without triethylamine (NEt_3) and H_2O at 25 ± 0.1 °C and an ionic strength of 0.01 M NaNO_3 . The reaction rate was found to be first-order with respect to CuL^4 complex and H_2L^n ligand. The rate of the ligand exchange reaction did not change significantly with the addition of H_2O to the DMF solvent; however, it increased when NEt_3 was added to the reaction mixture. The effect of NEt_3 and H_2O on the ligand exchange rate shows that the deprotonation/protonation of the H_2L^n ligand and anionic form of H_2L^n are essential to the reaction. A reaction mechanism is proposed and discussed for the effect of NEt_3 and H_2O on the ligand exchange rate.

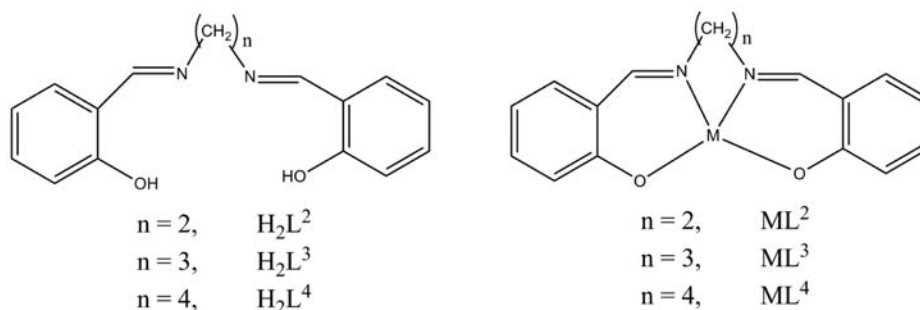
Keyword: Saturation kinetics, kinetic, ligand exchange, UV–Visible, Schiff base.

1. Introduction

The chemistry of the complexes of a salen type Schiff base, H_2L^2 (scheme 1), and its derivatives have been exhaustively studied to improve the coordination chemistry and because of their applications to modeling bioinorganic systems, catalysis, and analytical practice.^{1–8} Initial focus was on the synthesis and geometry of the salen complexes with bivalent metals. Gradually, research has moved toward synthesis and structural properties of the metal complexes of derivatives of salen with functional groups

and different chain lengths in the amine backbone (number of CH_2 groups, Scheme 1).^{9–12} The increase in the length of the methylene chain of the complexes allows sufficient flexibility in the structure by changing it from a planar to a distorted tetrahedral or forming species with a higher coordination number in the presence of additional donors.^{13–16}

Studies on the structure of the copper(II) complexes of salen and their derivatives have indicated that they are monomers and their flexibility results from an increase in chain length, which changes the geometry from square–planar to distorted tetrahedral.^{13–17} The increase in the



Scheme 1. A structural representation of the Schiff base ligands and complexes.

number of methylene units (n in the chain of H_2L^n , scheme 1) decreases the stability of the copper(II) complexes.¹⁸

This decrease in stability could be a driving force for the ligand exchange reaction and formation of a higher stable complex. In our previous study on the ligand exchange reactions,¹⁸ we investigated the kinetics and mechanism of the ligand exchange reaction between H_2L^2 and L^3 in the CuL^3 complex (reaction 1).



The present study investigates the kinetics of the ligand exchange reaction between H_2L^n ($n = 2, 3$) and L^4 in the CuL^4 complex (reactions 2 and 3).



2. Experimental

2.1. Reagents

Chemical reagents and all solvents, used in the syntheses and kinetic studies, were purified by standard methods.

The Schiff bases H_2L^n were prepared by a general method,^{18–20} the condensation reaction between 2 equivalents of salicylaldehyde and 1 equivalent of the appropriate diamine (1,2-ethylenediamine, 1,3-propanediamine and 1,4-butanediamine), in ethanol. The yellow products were obtained in yields typically 70% or better. Purity of products were verified by comparing with literature melting points (m.p.), 124, 53 and 90 °C for H_2L^2 , H_2L^3 and H_2L^4 , respectively.^{15–17}

The copper complexes were prepared by a general method,^{18,21,22} using the reaction solution of copper(II) acetate with the Schiff base ligand (1:1 molar ratio).

- **CuL²**: Yield 51%. Anal. Calculated for $C_{16}H_{14}CuN_2O_2$: C, 58.26; H, 4.28; N, 8.49. Found: C, 58.09; H, 4.23; N, 8.61.
- **CuL³**: Yield 50%. Anal. Calculated for $C_{17}H_{16}CuN_2O_2$: C, 59.38; H, 4.69; N, 8.15. Found: C, 59.12; H, 4.63; N, 8.21.
- **CuL⁴**: Yield 50%. Anal. Calculated for $C_{18}H_{18}CuN_2O_2$: C, 60.41; H, 5.07; N, 7.83. Found: C, 59.98; H, 5.13; N, 7.61.

2.2. Kinetics Measurements

The reaction of Schiff base H_2L^2 and H_2L^3 with a CuL^4 complex was studied under first order conditions using a GBC UV-Visible Cintra 101 spectrometer at 570 and 640 nm, respectively. This equals to the greatest change in molar absorptivity between reactants and products. The reaction mixture were made in dimethylformamide (DMF) solvent, $I = 0.01$ M $NaNO_3$, CuL^4 complex ($2.5 \times$

10^{-3} M) and different concentrations of Schiff base ligand with and without triethylamine, NEt_3 , and H_2O at 25 ± 0.1 °C. Equal volumes of the solution of the CuL^4 complex in DMF with the solution containing Schiff base (H_2L^2 or H_2L^3) ligand and $NaNO_3$ (with and without NEt_3 and H_2O) were mixed. The reaction mixture absorbance values were measured at defined times after mixing.

The pseudo-first-order rate constants (k_{obs}) were obtained from the plots of $-\ln(A_t - A_\infty)$ versus time, where A_t and A_∞ represent the absorbance of the reaction mixtures at time t and infinity, respectively. At each concentration an average of at least three kinetic runs was carried out and the rate constants (k_{obs}) were statistically averaged. Rate constant k was obtained by fitting the data to k_{obs} versus $[H_2L^n]$ using Sigmaplot 12.0.

3. Results and Discussion

3.1. Absorption Spectra

The visible absorption spectra of the CuL^2 , CuL^3 and CuL^4 complexes at equal concentrations in DMF solvent show maximum absorption due to d–d transition at 568, 605 and 642 nm, respectively (Fig. 1). The visible spectrum of the CuL^n complexes shows that the visible spectrophotometry easily followed the ligand exchange reaction. Fig. 2 shows a consecutive series of spectra recorded in DMF solvent for the CuL^4/H_2L^2 system (Fig. 2a) and CuL^4/H_2L^3 system (Fig. 2b) and shows a decrease in wavelength with respect to the starting CuL^4 spectrum. These observations indicate that the CuL^4 complex converted to a CuL^2 or CuL^3 complex (reactions 2, 3) when the H_2L^2 or H_2L^3 ligand, respectively, was added.

The spectrum produced by mixing equal amounts of CuL^2 or CuL^3 complex, H_2L^4 and $NaNO_3$ in DMF is similar to the last spectrum shown in Fig. 2. This similarity confirms the conversion of CuL^4 in the presence of H_2L^2 or H_2L^3 to a CuL^2 or CuL^3 complex, respectively.

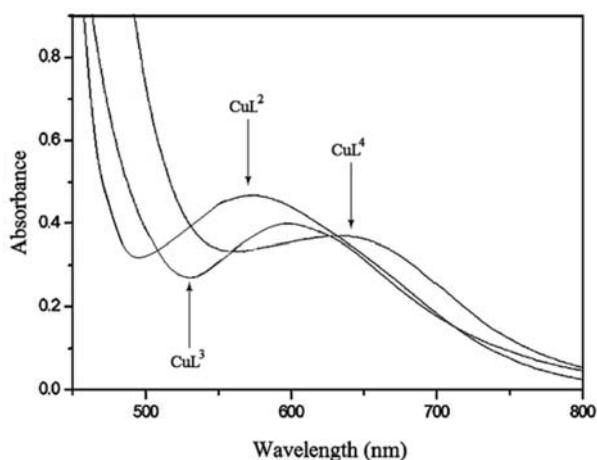


Figure 1. Visible spectra of CuL^n (2.5×10^{-3} M) complexes in DMF solvent.

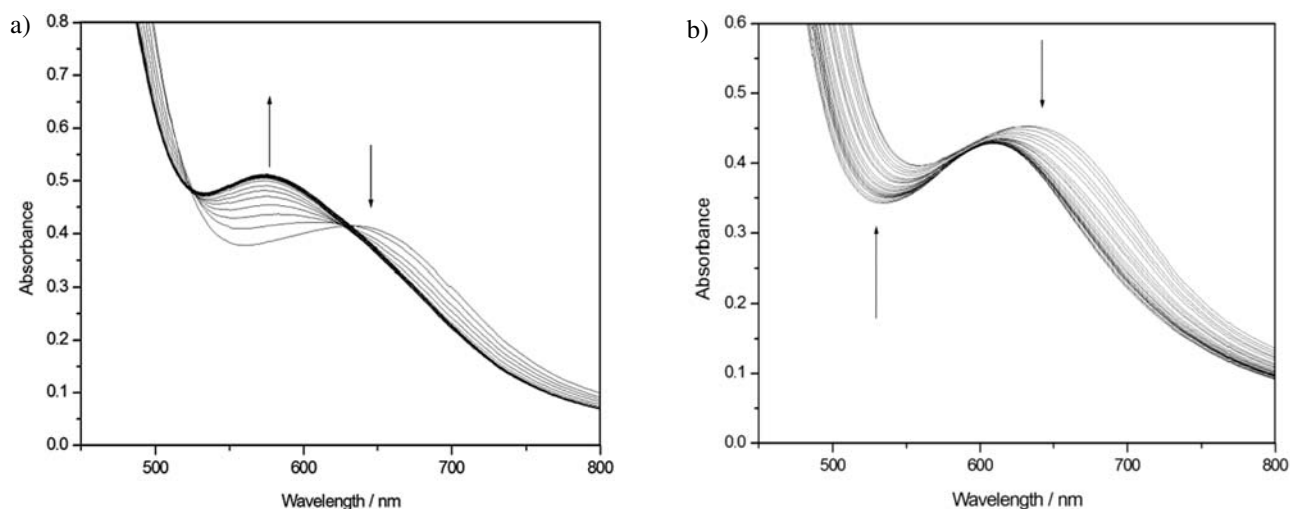


Figure 2. Spectral changes recorded in DMF solvent (a) for the reaction of CuL^4 (2.5×10^{-3} M) / H_2L^2 (2.5×10^{-3} M) (b) CuL^4 (2.5×10^{-3} M) / H_2L^3 (2.5×10^{-3} M).

3. 2. Kinetics Study

The reactions were monitored by following the increase in the 570 nm band for the $\text{CuL}^4/\text{H}_2\text{L}^2$ system and the decrease in the 640 nm band for the $\text{CuL}^4/\text{H}_2\text{L}^3$ system (Fig. 3) after mixing equal volumes of CuL^4 complex and H_2L^2 or H_2L^3 Schiff base ligand in DMF at $25 \pm 0.1^\circ\text{C}$. NaNO_3 was used to maintain the ionic strength at 0.01 M. All reactions were followed to at least 95% completion. Sample plots of the absorbance versus time data at 570 and 640 nm are shown in Fig. 3.

The rate constants (k_{obs}) of reaction 2 and 3 were obtained under pseudo-first-order conditions (Table 1). The rate law can be expressed in Eqs. 4 and 5:

$$\text{Rate} = -\frac{d[\text{CuL}^4]}{dt} = \frac{d[\text{CuL}^2]}{dt} = k_{\text{obs}} [\text{CuL}^4]_0 \quad (4)$$

$$\text{Rate} = -\frac{d[\text{CuL}^4]}{dt} = \frac{d[\text{CuL}^3]}{dt} = k_{\text{obs}} [\text{CuL}^4]_0 \quad (5)$$

The pseudo-first-order rate constants were measured at different ligand concentrations. The order of the reaction rate with respect to Schiff base ligand was determined by plotting k_{obs} as a function of ligand concentration. Fig. 4 shows the variation in k_{obs} versus Schiff base ligand concentration, illustrating the saturation kinetics (see proposed mechanism).

The conversion of CuL^4 by adding H_2L^2 or H_2L^3 Schiff base ligand to CuL^2 and CuL^3 , respectively, in DMF solvent showed that they were thermodynamically more stable than the CuL^4 complex. To confirm this, the reverse of reactions 2 and 3, i.e., the conversion of CuL^2 or CuL^3 when adding H_2L^4 ligand to the CuL^4 does not take place. In this condition, a reverse

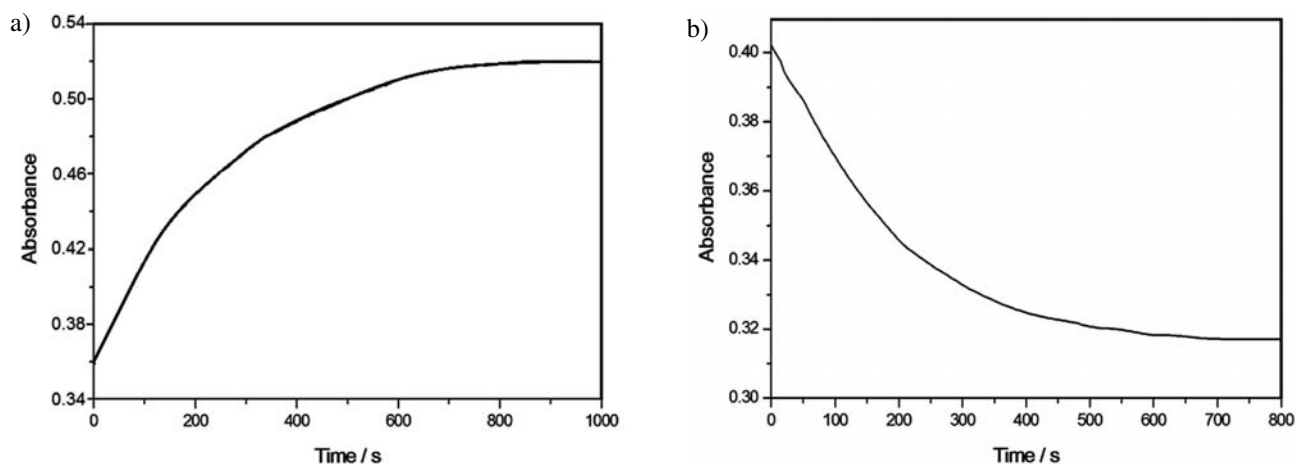
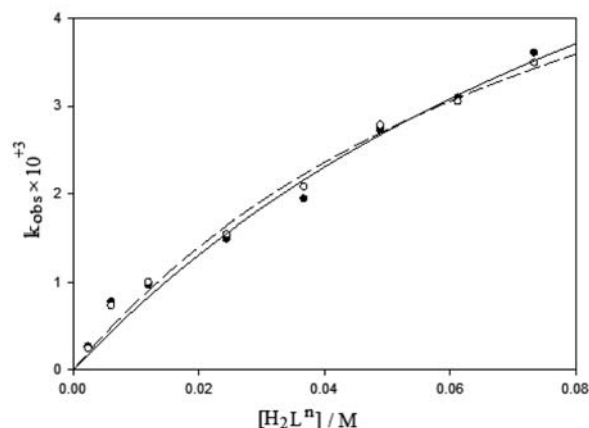


Figure 3. Plot of absorbance vs. time for the typical ligand exchange reaction (A) $\lambda = 570$ nm for CuL^4 (2.5×10^{-3} M) / H_2L^2 (2.5×10^{-3} M), (B) $\lambda = 640$ nm for CuL^4 (2.5×10^{-3} M) / H_2L^3 (2.5×10^{-3} M) in DMF solvent.

Table 1 Rate data for the reaction of CuL^4 (0.0025 M) with H_2L^n (0.025 M) ligand in the presence of variable $[\text{NEt}_3]$

$[\text{NEt}_3] / \text{M}$	H_2L^2	H_2L^3
	$k_{\text{obs}} \times 10^4 / \text{s}^{-1}$	$k_{\text{obs}} \times 10^4 / \text{s}^{-1}$
0	1.49 ± 0.10	1.88 ± 1.15
0 ^a	1.48 ± 0.12	1.90 ± 1.13
0.0018	2.67 ± 0.15	3.12 ± 0.14
0.0036	3.19 ± 0.14	3.71 ± 0.15
0.0054	3.35 ± 0.17	5.21 ± 0.11
0.0072	3.56 ± 0.11	6.18 ± 0.17
0.009	3.13 ± 0.14	4.62 ± 0.16
0.011	3.56 ± 0.16	7.76 ± 0.11
0.013	3.89 ± 0.17	8.50 ± 0.13
0.014	3.98 ± 0.19	9.51 ± 0.18

^a in the presence of H_2O (0.56 M)**Figure 4.** Plots of k_{obs} vs. $[\text{H}_2\text{L}^n]$ for ligand exchange reaction of L^4 in CuL^4 by H_2L^2 in the absence H_2O (●) and in the presence H_2O (○)

reaction and equilibrium cannot be observed between the two complexes.

The H_2L^2 Schiff base ligand with the ion Cu(II) formed a square-planar complex only slightly distorted

from planarity.^{15–17} Increasing the number of methylene units in the chain of the Schiff base ligand (Scheme 1) provided enough flexibility in CuL^3 and CuL^4 to invert it from a planar configuration (CuL^2) to a distorted tetrahedral (CuL^3) or tetrahedral (CuL^4) configuration; the dihedral angles are 12.2, 25.4 and 42.6°, respectively.^{17,18}

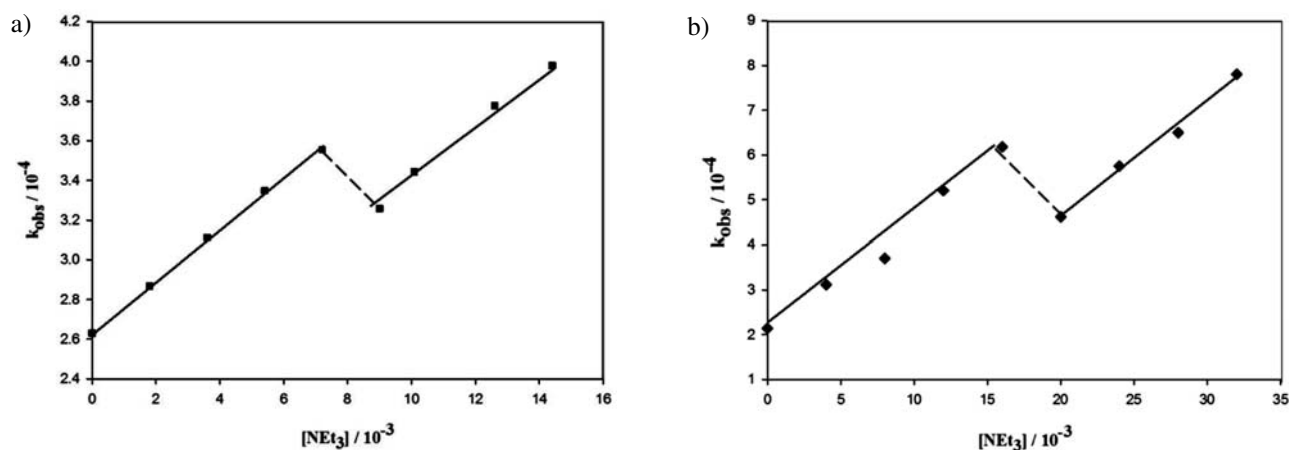
Distortion about the copper center of the CuL^4 complex from the extra methylene group decreased the ligand field strength. In addition, the L^4 with Cu(II) forms a larger chelate ring (seven-membered) than the CuL^2 and CuL^3 complexes (five- and six-membered, respectively). The effect of size of the chelate ring on complex stability has been reported elsewhere.^{17, 23–25} The complex stability decreased as the chelate ring size increased. The seven-membered chelate ring led to less stable complexes than the six- and five-membered chelate rings.

The decrease in ligand field strength and stability of CuL^4 and CuL^3 relative to CuL^2 are in accord with the trend observed in the ligand exchange reactions (reactions 2 and 3). This is consistent with previous our resulted on kinetics of ligand exchange in the $\text{CuL}^3/\text{H}_2\text{L}^2$ system (reaction 1).¹⁸

The kinetics of the reaction was investigated in the presence of NEt_3 and/or H_2O to propose a mechanism for this exchange reaction.

3. 3. Effect of Triethylamine

The rate of the exchange reaction increased when NEt_3 was added to the reaction mixture. The reaction was carried out at different NEt_3 concentrations, which indicates that the ligand exchange strongly depends on NEt_3 concentration. The reaction rate increased considerably as the NEt_3 concentration increased relative to the reaction in the absence of NEt_3 (Fig. 5). There is an obvious break in the plot of k_{obs} versus $[\text{NEt}_3]_0$ at NEt_3 concentrations of $\sim 0.007\text{--}0.009$ M in the $\text{CuL}^4/\text{H}_2\text{L}^2$ system (Fig. 5a) and

**Figure 5.** Plots of k_{obs} vs. $[\text{NEt}_3]$ for ligand exchange reaction (a) the system $\text{CuL}^4 / \text{H}_2\text{L}^2$ (b) $\text{CuL}^4 / \text{H}_2\text{L}^3$.

~0.015–0.020 M in the $\text{CuL}^4/\text{H}_2\text{L}^3$ system (Fig. 5b). This can be attributed to the change in reaction species at these concentrations of NEt_3 .

3. 4. Reaction in Presence of H_2O

The plot of k_{obs} versus $[\text{H}_2\text{L}^n]$ in the presence and absence of H_2O is shown in Fig. 4. It indicates that the rate of the ligand exchange reactions (reactions 2 and 3) did not change considerably when H_2O (0.56 M) was added to the DMF. The ligand exchange reaction rate in the presence of NEt_3 , however, considerably decreased when H_2O (0.56 M) was added to the reaction solution (Table 1). The effects of NEt_3 and H_2O show the importance of protonation/deprotonation in the rate of the ligand exchange reaction.

3. 5. Proposed Mechanism

Fig. 2 shows two isosbestic points at 532 and 622 nm for the $\text{CuL}^4/\text{H}_2\text{L}^2$ system (Fig. 2a) and one isosbestic point at 598 nm for the $\text{CuL}^4/\text{H}_2\text{L}^3$ system (Fig. 2b). This indicates that CuL^4 converted to CuL^2 or CuL^3 without the formation of a free Cu^{2+} ion,^{26–28} which has a different spectrum from the CuL^n complexes. In general, the ligand exchange reaction between polydentate ligands proceeds via intermediates where the incoming ligand is partially coordinated to the metal center and the leaving ligand is partially dissociated.^{27,28}

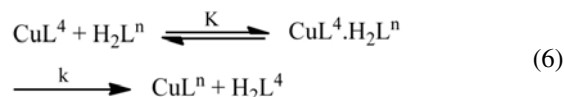
The acidity of H_2L^n and its family Schiff base ligands was low,²⁹ thus, deprotonating the Schiff base ligands did not take place in the absence of a base. This assumption was confirmed by the ligand exchange reaction in the presence of H_2O with no changes in reaction rate (Fig. 4 and Table 1).

Fig. 4 shows a representative graph for k_{obs} dependence on the free ligand in the absence and presence of H_2O . It shows saturation kinetic dependence on the free ligand and zero intercepts at the extrapolated zero concentration. The zero intercept confirms the negligible contribution of solvent to the overall rate.

Saturation kinetics indicates that a limiting value of k_{obs} was reached at high [ligand]. The rate increased as the $[\text{H}_2\text{L}^n]$ increased before the limiting value (Fig. 4), which is probably caused by the formation of the outer sphere

association complex. At this stage, the interchange of ligands from outer sphere to inner sphere occurs, i.e., H_2L^n attacks the $\text{Cu}(\text{II})$ atom to produce an intermediate complex ($\text{CuL}^4 \cdot \text{H}_2\text{L}^n$, $n = 2$ and 3).

This suggests production of a formation species from the association between CuL^4 and the Schiff base ligand prior to ligand exchange (reaction 6, $n = 2, 3$).



The theoretical rate law can be given as Eq. 7:

$$k_{\text{obs}} = \frac{kK[\text{H}_2\text{L}^n]}{1 + K[\text{H}_2\text{L}^n]} \quad (7)$$

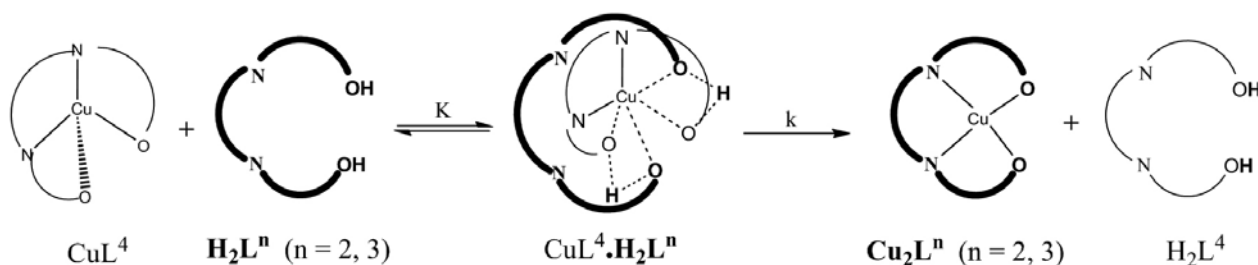
where K is the equilibrium constant between the CuL^4 complex and H_2L^n ($n = 2, 3$) ligand and k is the rate constant of the ligand exchange reaction.

Displacement of H_2L^n from the $\text{Cu}(\text{II})$ complexes likely involves the initial coordination of H_2L^n oxygen groups to the copper center in the CuL^4 complex followed by proton–transfer from H_2L^n to the L^4 ligand in the CuL^4 complex ($\text{CuL}^4 \cdot \text{H}_2\text{L}^n$), with the bond cleavage of the two-end L^4 ligand. The reaction is completed by replacing L^4 with H_2L^n . (scheme 2).

Fitting Eq. 7 with the experimental data yields $k = (9.50 \pm 0.28) \times 10^{-3} \text{ s}^{-1}$ (in $\text{CuL}^4/\text{H}_2\text{L}^2$ system) and $k = (2.93 \pm 0.16) \times 10^{-2} \text{ s}^{-1}$ (in $\text{CuL}^4/\text{H}_2\text{L}^3$ system).

The k values are in the same order separately in the presence and absence of H_2O at the base Schiff ligands (Fig. 4). This is in agreement with the assumption of H_2L^n being a major reaction species. In this case, no species deprotonation or protonic equilibrium was expected for H_2L^n under the reaction conditions.

Fig. 6 shows a consecutive series of spectra recorded in DMF solvent for the reaction of CuL^4 with H_2L^2 in the presence of NEt_3 . The absorption spectra indicate shifted towards a smaller λ with respect to the starting CuL^4 spectrum, which is similar to Fig. 2. The changes observed in the spectrum indicate that, in the presence of NEt_3 , the CuL^4 complex was converted to a CuL^2 complex with the addition of the H_2L^2 ligand.



Scheme 2. The suggest mechanism for ligand exchange reaction in the system $\text{CuL}^4/\text{H}_2\text{L}^n$.

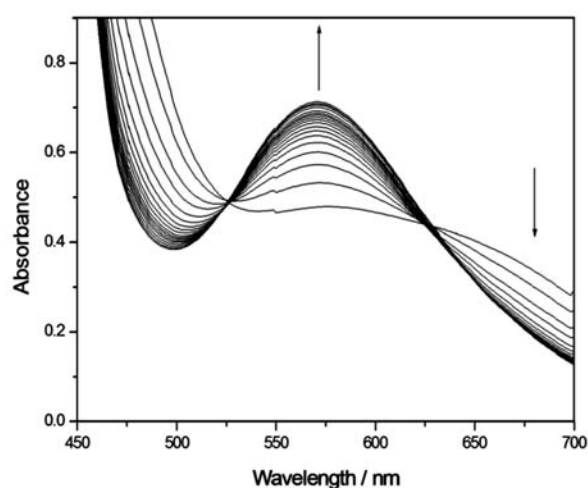


Figure 6. Spectral changes recorded in DMF solvent for the reaction of CuL^4 (2.5×10^{-3} M) / H_2L^2 (2.5×10^{-3} M) and NEt_3 (1.8×10^{-3} M).

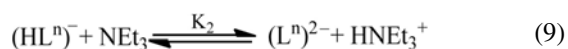
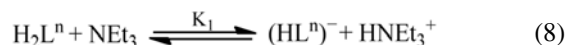
As shown in Fig. 5 and Table 1, the ligand exchange rate increased when NEt_3 was added. The effect of NEt_3 could be its interaction with either CuL^4 or the H_2L^n ligand. The spectrum of the CuL^4 complex in the presence or absence of NEt_3 in DMF did not change; thus, adduct formation between NEt_3 and CuL^4 was not observed. The absorption spectrum of the H_2L^n ligand changed as NEt_3 increased.

The dependence of the reaction rate on the concentration of NEt_3 can only be explained by the deprotonated H_2L^n ligand.¹⁸ As $[\text{NEt}_3]$ increased, the anionic form of H_2L^n ($(\text{HL}^n)^-$ and $(\text{L}^n)^{2-}$) increased significantly, which was reflected in the rate constant values.

The ligand exchange rate increased when NEt_3 was added and the reaction rate decreased when H_2O was added to the reaction mixture in the presence of NEt_3 . There was a break in the plot of k_{obs} versus [in the presence of

NEt_3 (Fig. 5) which suggests that $(\text{HL}^n)^-$ ions are major reactive species in the presence of NEt_3 . Under these reaction conditions, at a relatively low $[\text{NEt}_3]$, the $(\text{HL}^n)^-$ ion is the main reactive species and, at high $[\text{NEt}_3]$, the $(\text{L}^n)^{2-}$ ion is the main reactive species.¹⁸ This suggests that an acceptable mechanism in the presence of NEt_3 is provided by scheme 3:

In the first step, NEt_3 quickly produced labile $(\text{HL}^n)^-$ and $(\text{L}^n)^{2-}$ ions (depending on NEt_3 concentration) by the deprotonation of proton(s) from the phenolic group(s) of H_2L^n (Eqs. 8 and 9).

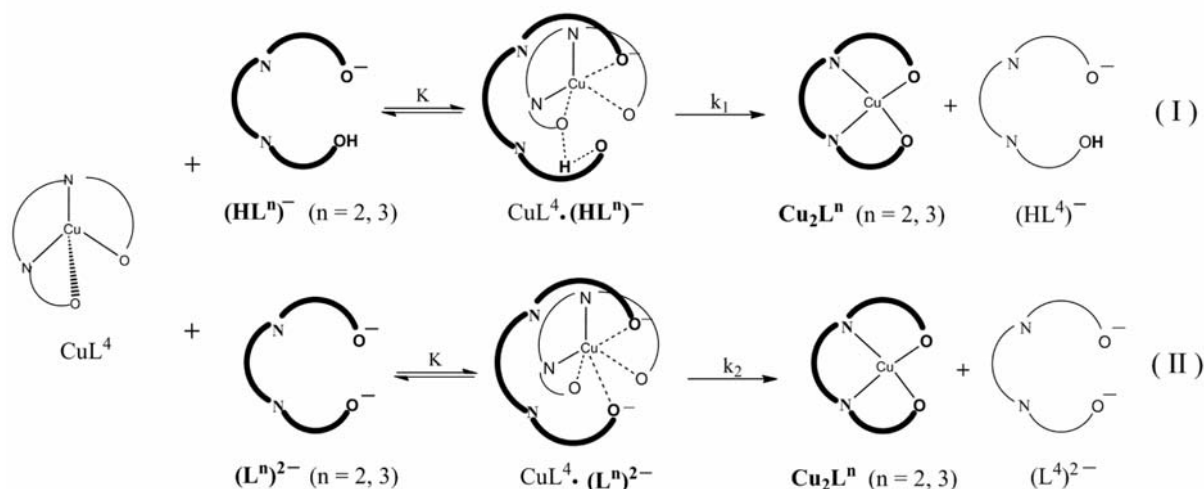


The coordination of the oxygen group of the $(\text{HL}^n)^-$ (path 1) or $(\text{L}^n)^{2-}$ (path 2) with the copper center in the CuL^4 complex was followed intramolecular proton transfer from $(\text{HL}^n)^-$ to L^4 (path 1). The bond cleavage of the two-end L^4 and ligand exchange was completed, as in the reaction without NEt_3 .

Using the proposed mechanism the rate law of ligand exchange can be expressed as:

$$k_{\text{obs}} = \frac{k_1[(\text{HL}^n)^-] + k_2[(\text{L}^n)^{2-}]}{[(\text{HL}^n)^-] + [(\text{L}^n)^{2-}]} \quad (10)$$

At low NEt_3 concentrations, the Eq. 8 was the main reaction and the $(\text{HL}^n)^-$ ion was the active species in the ligand exchange reaction. Under this condition, Eq. 10 is assumed to convert to $k_{\text{obs}} \approx k_1$. At high NEt_3 concentrations, interaction between the $(\text{HL}^n)^-$ ion and NEt_3 produced a $(\text{L}^n)^{2-}$ ion (Eq. 9), allowing Eq. 10 to be simplified to $k_{\text{obs}} \approx k_2$. Fig. 5 shows that the slope of plot k_{obs} versus $[\text{NEt}_3]$ for a high $[\text{NEt}_3]$ was less than that for a low $[\text{NEt}_3]$. It can then be assumed that, in Eq. 10, $k_2 < k_1$.



Scheme 3. The suggest mechanism for ligand exchange reaction in the system $\text{CuL}^4 / \text{H}_2\text{L}^n$ in the present of NEt_3 .

The rate of the ligand exchange reaction was dependent on the NEt_3 concentration such that increasing the NEt_3 concentration increased the rate of the reaction because the concentration of the $(\text{HL}^n)^-$ ion increased. The $(\text{HL}^n)^-$ ion quickly coordinates with the Cu center from the oxygen phenolic group, followed by bond cleavage of L^4 in the CuL^4 complex by intramolecular proton transfer from $(\text{HL}^n)^-$ to L^4 . At high NEt_3 concentrations, the $(\text{HL}^n)^-$ produced from reaction 8 was deprotonated and converted to an $(\text{L}^n)^{2-}$ ion (Eq. 9). The $(\text{L}^n)^{2-}$ quickly coordinated with the Cu complex, but the $(\text{L}^n)^{2-}$ ion cannot quickly rebounded for bond cleavage of L^4 in the CuL^n complex and the rate of the ligand exchange reaction decreased relative to the reaction at low $[\text{NEt}_3]$. This created the observed break in plot k_{obs} versus $[\text{NEt}_3]$ from the decrease in the concentration of the $(\text{HL}^n)^-$ ion with the increase in $[\text{NEt}_3]$.

The ligand exchange rate in the presence of NEt_3 decreased when H_2O was added which is likely the result of the protonation of the $(\text{HL}^n)^-$ and $(\text{L}^n)^{2-}$ ions. The protonated species of $(\text{HL}^n)^-$ and $(\text{L}^n)^{2-}$ ions formed a H_2L^n ligand and the ligand reaction rate decreased. These experimental observations confirm that the deprotonated/protonated H_2L^n ligand and anionic form of H_2L^n was essential to the ligand exchange reaction.

4. Conclusion

Distortion about the Cu(II) in CuL^n complex was caused by the formation a larger chelate ring which creates a less stable complex than the CuL^n complex. This effect was the driving force for replacing the H_2L^n ($n = 2$ and 3) ligand with L^4 in the CuL^4 complex. The ligand exchange reaction was investigated for the presence or absence of NEt_3 and H_2O in the DMF solvent. The reaction rate did not change when H_2O was added; however, in the presence of NEt_3 , the ligand exchange reaction rate increased in response to the deprotonation of the H_2L^n ligand. These observations confirm that the deprotonation/protonation of the H_2L^n ligand and the anionic form of the ligand are essential to the ligand exchange reaction.

5. Acknowledgments

The authors are grateful to the Yazd University for partial support of this work.

6. Reference

1. T. P. Camargo, R. A. Peralta, R. Moreira, E. E. Castellano, A. J. Bortoluzzi, A. Neves, *Inorg. Chem. Commun.* **2013**, *37*, 34–38.
2. F. Dehghani, A. R. Sardarian, M. Esmailpour, *J. Organomet. Chem.* **2013**, *43*, 87–96.
3. S. Carradori, C. D. Monte, M. D. Ascenzio, D. Secci, G. Celik, M. Ceruso, D. Vullo, A. Scozzafava, C. T. Supuran, *Bioorg. Med. Chem. Lett.* **2013**, *23*, 6759–6763.
4. A. M. Ajlouni, Z. A. Taha, W. A. Momani, A. K. Hijazi, M. Ebqaai, *Inorg. Chim. Acta* **2012**, *388*, 120–126.
5. M. N. Dehkordi, A. K. Bordbar, P. Lincoln, V. Mirkhani, *Spectrochim. Acta A* **2012**, *90*, 50–54.
6. M. Mariappan, M. Suenaga, A. Mukhopadhyay, B. G. Maiya *Inorg. Chim. Acta*, **2012**, *390*, 95–104.
7. F. J. Fard, Z. M. Khoshkhoo, H. Mirtabatabaei, M. R. Housaindokht, R. Jalal, H. E. Hosseini, M. R. Bozorgmehr, A. A. Esmaili, M. J. Khoshkholgh, *Spectrochim. Acta A* **2012**, *97*, 74–82.
8. Z. A. Taha, A. M. Ajlouni, K. A. Al-Hassan, A. K. Hijazi, A. B. Faiq, *Spectrochim. Acta A* **2011**, *81*, 570–577.
9. N. Saravanan, M. Palaniandavar, *Inorg. Chim. Acta* **2012**, *385*, 100–111.
10. M. Izakovic, J. Sima, *Acta Chim. Slov.* **2004**, *51*, 427–436.
11. M. Asadi, H. Sepehrpour, K. Mohammadi, *J. Serb. Chem. Soc.* **2011**, *76*, 63–74.
12. M. Dieng, I. Thiam, M. Gaye, A.S. Sall, A.H. Barry, *Acta Chim. Slov.* **2006**, *53*, 417–423.
13. R. Vafazadeh, B. Khaledi, A.C. Willis, M. Namazian, *Polyhedron* **2011**, *30*, 1815–1819.
14. R. Vafazadeh, B. Khaledi, A.C. Willis *Acta Chim. Slov.* **2012**, *59*, 954–958.
15. J. Reglinski, S. Morris, D. E. Stevenson, *Polyhedron* **2002**, *21*, 2167–2174.
16. J. Reglinski, S. Morris, D. E. Stevenson, *Polyhedron* **2002**, *21*, 2175–2182.
17. L. C. Nathan, J. E. Koehne, J. M. Gilmore, K. A. Hannibal, W. E. Dewhirst, T. D. Mai, *Polyhedron* **2003**, *22*, 887–894.
18. R. Vafazadeh, S. Bidaki, *Acta Chim. Slov.* **2010**, *57*, 310–317.
19. R. Vafazadeh, M. Hatefi-Ardakani *Bull. Korean Chem. Soc.* **2006**, *27*, 1685–1688.
19. R. Vafazadeh, M. Kashfi, M. *Bull. Korean Chem. Soc.* **2007**, *28*, 1227–1230.
20. R. Vafazadeh, V. Hayeri, A. C. Willis, *Polyhedron* **2010**, *29*, 1810–1815.
21. R. Vafazadeh, R. Esteghamat-Panaha, A. C. Willis, A. F. Hill, *Polyhedron* **2012**, *48*, 51–57.
22. R. D. Hancock, A. E. Martell, *Chem. Rev.* **1989**, *89*, 1875–1914.
23. R. D. Hancock, *Acc. Chem. Res.* **1990**, *23*, 253–257.
24. B. Wang, C. S. Chung, *J. Chem. Soc. Dalton Trans.* **1982**, 2565–2566.
25. R. G. Wilkins, *Kinetics and Mechanism of Reactions of Transition Metal Complexes*, Wiley, New York, **1986**, p.p. 156–159
26. H. Elias, S. Schwartze-Eidam, K. J. Wannowius, *Inorg. Chem.* **2003**, *42*, 2878–288.
27. G.V. Rao, R. Bellam, N. R. Anipindi, *Transition Met. Chem.* **2012**, *37*, 189–196.
28. N. Hirayama, I. Takeuchi, T. Honjo, K. Kubono, H. Kokuken, *Anal. Chem.* **1997**, *69*, 4814–4818.

Povzetek

Kinetika izmenjave ligandov v sistemu $\text{CuL}^4/\text{H}_2\text{L}^n$, kjer je H_2L^n N,N' -alkilen-bis(salicildimin) tetradentatni ligand Schiffove baze ($n = 2$ ali 3 ; število CH_2 skupin v verigi aminskega ogrodja) je bila proučevana spektrofotometrično v DMF v prisotnosti ali brez trietilamina (NEt_3) in H_2O pri 25 ± 0.1 °C, pri ionski jakosti raztopine $0,01$ M NaNO_3 . Reakcija izmenjave ligandov je prvega reda glede na kompleks CuL^4 in H_2L^n ligand. Hitrost reakcije izmenjave ligandov se bistveno ne spremeni ob dodatku H_2O k topilu DMF, medtem ko se hitrost poveča ob dodatku NEt_3 k reakcijski zmesi. Vpliv dodatkov NEt_3 in H_2O na hitrost izmenjave ligandov kaže, da je proces deprotonacije/protonacije liganda H_2L^n in njegove anionske oblike bistvenega pomena za to reakcijo. Predlagan je mehanizem reakcije izmenjave ligandov in obravnavan vpliv NEt_3 in H_2O na hitrost izmenjave ligandov.